Carbochlorination of Dispersed Oxides in a Molten Salt Reactor

Reaction mechanism and rates were determined from 803 to 1,073 K for the carbochlorination of Al_2O_3 and of Al, Si and Fe-mixed oxides using Cl_2 and C slurried in a stirred melt of NaCl—$AlCl_3$. Alumina chlorination rates of 0.33-2.0 × 10^{-8} kmol/s were obtained using C:melt weight ratios between 1:21 and 1:42. The reaction rate was proportional to C loading at temperatures below 923 K, while gas-liquid mass transfer was rate-controlling at higher temperatures. Carbochlorination of the combined oxides in coal fly ash at 923 K and oxide conversions less than about 50% was also gas-liquid mass-transfer-controlled. At higher conversions, dissolution became the rate-controlling factor. A 40% (molar) $AlCl_3$ melt was more effective than a 48% $AlCl_3$ melt for the selective chlorination of Al_2O_3 over SiO_2.

Michael S. Dobbins,
George Burnet
Ames Laboratory, U.S.D.O.E., and
Department of Chemical Engineering
Iowa State University
Ames, IA 50011

Introduction

The conversion of metal oxides to chlorides is typically carried out in the presence of both reducing and chlorinating agents. Carbon and CO are the most common reductants, thus the term carbochlorination, although S has also been used (Milne and Holliday, 1975). The overall carbochlorination of Al_2O_3 in the absence of other metal oxides is described by Eqs. 1 and 2:

$$Al_2O_3 + 3Cl_2 + 3C \rightarrow 2AlCl_3 + 3CO \qquad (1)$$

$$Al_2O_3 + 3Cl_2 + 3CO \rightarrow 2AlCl_3 + 3CO_2 \qquad (2)$$

Reactions 1 and 2 are often combined into a single reaction to show that CO_2 is the principal gaseous product:

$$2Al_2O_3 + 6Cl_2 + 3C \rightarrow 4AlCl_3 + 3CO_2 \qquad (3)$$

Analogous gas-solid reactions occur when other metal oxides are present. The reductant and chlorinating agent may also be combined in a single compound, such as $COCl_2$ or CCl_4.

Prior work on the carbochlorination of mixed oxide materials has focused on gas-solid reaction systems (Bombara and Tanzi, 1984; Burnet et al., 1984; Adelman and Burnet, 1987). When solid reductants are used, these systems are rate-limited by the need for physical contact between the reductant and the oxides. Gaseous reductants eliminate the problem of physical contact, but are less effective in promoting chlorination. The carbochlorination of low surface area oxides shows similar behavior.

This paper deals with the carbochlorination of pure and mixed oxides using a technique proposed by Haupin and Remper (1977) for low surface area Al_2O_3. The carbochlorination takes place in a slurry consisting of the oxide and C in a NaCl—$AlCl_3$-fused salt, which is an extension of earlier work by Hille and Durrwachter (1960) proposing the use of NaCl as a catalyst for the oxide/Cl_2 reaction.

Seon et al. (1983), using electrochemical techniques, monitored the formation of reaction intermediates in a fused salt carbochlorination reaction. A study of the chlorination of Al_2O_3 using $COCl_2$ in a KCl—LiCl eutectic disclosed that the Al_2O_3 dissolved in the melt as $AlOCl_2^-$ by the reaction:

$$Al_2O_3(s) + 4Cl^- \leftrightarrow 2AlOCl_2^- + O^{2-} \qquad (4)$$

The dissolved oxide subsequently reacted with the $COCl_2$ to form $AlCl_3$ and CO_2. The dissolution reaction thus virtually eliminated the effect of surface area on the reaction rate by converting solid Al_2O_3 to a solute. It was also observed that $AlCl_3$ dissolved in the melt causes a further increase in Al_2O_3 solubility (Tremillion et al., 1976; Seon et al., 1983) by the reaction:

$$AlCl_4^- + O^{2-} \leftrightarrow AlOCl_2^- + 2Cl^- \qquad (5)$$

Mixtures of dissimilar metal oxides and fused metal chlorides may also undergo an exchange reaction. Equation 6 shows the

---

Correspondence concerning this paper should be addressed to M. S. Dobbins, Research and Development Division, Corning Glass Works, SPDV020, Corning, NY 14831.

reaction of $AlCl_3$ with Fe_2O_3:

$$Fe_2O_3 + 2AlCl_3 \rightarrow 2FeCl_3 + Al_2O_3 \qquad (6)$$

Thus, in the presence of a large excess of $AlCl_3$, which is thermodynamically less stable than most other chlorides, the chlorination reaction can occur by two distinct paths—the carbochlorination reactions (Eqs. 1 and 2) and the chloride exchange reaction (Eq. 6). In NaCl—$AlCl_3$ melts, all the common metal oxides, except for silica, are thermodynamically favored to react with $AlCl_3$ via reactions of the form of Eq. 6. Alumina formed by the exchange reactions is subsequently dissolved in the melt and carbochlorinated.

To test the feasibility of chlorinating mixed oxides in a fused salt slurry, a reactor system was developed that is capable of operating at temperatures as high as 1,073 K. Means for sampling the reactor contents and monitoring the composition of the noncondensable gas products as a function of time were incorporated. Chlorination of pure Al_2O_3 permitted investigation of the carbochlorination reaction with respect to temperature, C loading and other parameters, without having to account for changes in mixed oxide reactivity and composition, as a function of conversion.

The chlorination rate of Al_2O_3 was found to be independent of its loading in the slurry, indicating that the rate of dissolution was faster than that of reaction. The reaction rate was not substantially effected by melt composition in the range of compositions tested or by the Cl_2 flow rate.

The reaction of alumina was found to be proportional to the C loading at temperatures below 873 K, with an observed activation energy of 121 kJ/kmol. At temperatures in excess of 973 K, gas-liquid mass transfer became the rate-limiting factor and the activation energy was 29.3 kJ/kmol. A local maximum in the reaction rate between 873 and 923 K was observed along with an increase in the $CO:CO_2$ ratio, providing strong experimental support for the presence of $COCl_2$ as a key reaction intermediate.

In contrast to Al_2O_3, the chlorination of power plant fly ash, selected as a naturally occurring mixed oxide, was strongly affected by the melt composition and the reactivity of individual components in the ash. A $48\%_m$ $AlCl_3$ content melt was more aggressive towards the chlorination of SiO_2 than a $40\%_m$ $AlCl_3$ melt with a corresponding loss of selectivity between the conversion of Al_2O_3 and SiO_2. The ratio of Al_2O_3 to SiO_2 conversion was 2.55 for the $48\%_m$ $AlCl_3$ melt compared to 5.46 for the $40\%_m$ $AlCl_3$ melt. In addition, the $40\%_m$ $AlCl_3$ melt afforded a faster initial rate of reaction as determined by analysis of the partially reacted oxide.

In summary, carrying out the carbochlorination of finely divided metal oxides in a fused salt slurry was found to facilitate both reaction and control. A disadvantage could be the need to handle a corrosive, hygroscopic fused salt at high temperatures.

Equipment and Procedures

The experimental equipment and procedures have been detailed elsewhere (Dobbins and Burnet, 1984; Dobbins, 1986), so only a brief overview is presented here. The chlorination equipment consisted of the reactor, two chloride condensers, and a gas chromatograph for noncondensable product gas analysis. A flow diagram of the system is shown in Figure 1.

Reaction rates of individual oxide species were monitored by sampling the slurry, while Cl_2 conversion was determined from analysis of the reactor product gas. Carbon conversion data were obtained from slurry samples and from product gas analyses. Chlorination of a pure oxide (Al_2O_3) did not require slurry sampling, since all the rate data were obtainable from product gas analyses.

The reactor was approximately 50 cm high and 7 cm in diameter, and was constructed of fused SiO_2 to resist corrosion by the NaCl—$AlCl_3$ melt. The lower half of the reactor was heated using a tube furnace; the working depth of slurry in the reactor was approximately 10 cm. The slurry was kept in suspension using a paddle stirrer constructed from fused SiO_2 and 316 stainless steel. Chlorine was injected into the slurry beneath the stirrer and as close to the reactor bottom as possible to promote gas distribution. The sparger consisted of a 6-mm diameter, closed-end tube, with three 3-mm holes placed at the base of the tube, equidistant about the circumference.

A sampler based on a device reported by Bamberger (1975) was used to sample the reactor contents during a run. Two-gram

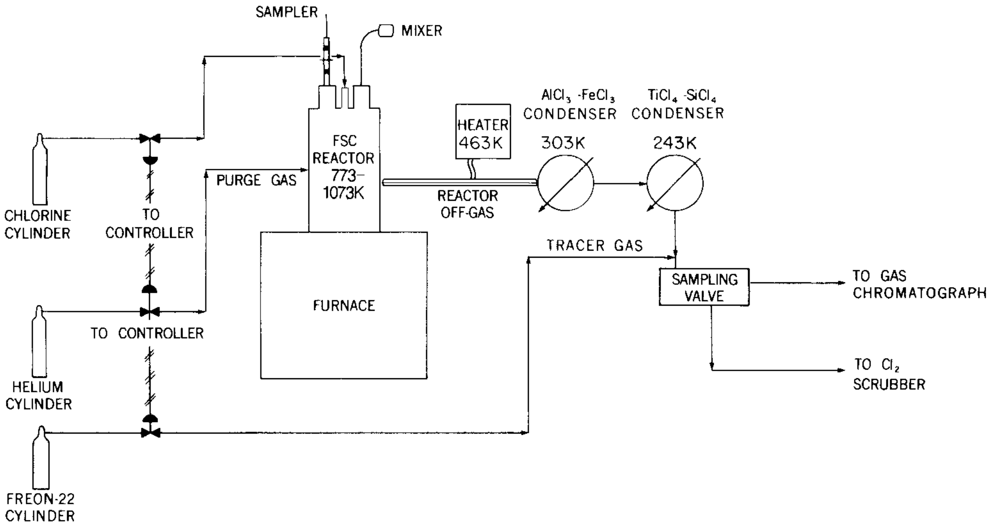

Figure 1. Fused salt chlorination equipment flow diagram.

samples of the slurry were taken at 15-minute intervals and were analyzed using standard methods (Dobbins, 1986).

Vaporized metal chlorides exiting the reactor along with CO_2, CO, He, and unreacted Cl_2 were removed from the product gas stream by two-stage condensation. The cooled product gas was analyzed for Cl_2, CO_2, and CO using a Hewlett-Packard 5750 gas chromatograph equipped with a thermal conductivity detector and 4.6 m × 0.003 m Teflon column packed with $10\%_w$ H_3PO_4 coated on 60/80 Carbopack B (Supelco). To determine the chlorination rate from the product gas analysis, the total gas flow rate was also required. Freon-22 was injected as a tracer into the cooled product gas at a known rate and its concentration used to back-calculate the flow rate.

The slurry used in the experiments contained 375 g of the NaCl—$AlCl_3$ salt mixture and 1 g of $BaCl_2$, which is nonvolatile at the temperatures used. Changes in the mass of salt in the reactor due to volatilization and other losses were calculated from changes in the $BaCl_2$ content of the slurry samples. Changes of less than 5% were typical over the course of a 2.5-hour chlorination. The solids loading of the slurry depended on the experimental conditions and varied from 4.2 to 40 g and from 25 to 80 g for the C and metal oxides, respectively.

The Al_2O_3 used in the study was produced by calcining Fisher $Al(OH)_3$ overnight at 973 K. The surface area of the material was 10^5 m^2/kg, which is typical of Al_2O_3 produced by low-temperature calcination. The mixed oxide was a fly ash derived from combustion of a Pennsylvania #6 coal. The original ash was commercially processed by the Halomet Corporation, Masontown, PA, to remove a magnetic fraction of the ash as a substitute magnetite. A 2-kg sample of the nonmagnetic ash was subsequently sieved to obtain a −325 mesh fraction required to limit settling in the reactor. The C source was pulverized metallurgical-grade coke obtained from a local foundry. B.E.T. measurements of the three different coke samples used in this work gave surface areas of 3.03×10^3, 8.75×10^3 and 5.22×10^3 m^2/kg. The three batches were used in the Plackett-Burman, temperature and mixed oxide chlorinations respectively.

Results and Discussion

Alumina chlorination

The effects of temperature, melt composition, melt: Al_2O_3 ratio, melt:C ratio, and Cl_2 flow rate were screened using the Plackett-Burman experimental design method. The method determines the individual effect of three or more process parameters but does not detect interactions among variables.

Table 1 shows the two levels used for each parameter tested. Temperatures were selected from results of previous work on the development of the experimental system (Dobbins and Burnet, 1984), while the melt compositions were determined from the liquids and boiling point compositions of NaCl—$AlCl_3$ melts at 1,073 K. The salt:Al_2O_3 ratios were derived from Al_2O_3 loadings of 50 and 25 g. Carbon loadings were based on a 1:1 stoichiometry between the Al_2O_3 and C at the high Al_2O_3 and high C loadings, assuming the formation of CO only (Eq. 1). In reality, the high Al_2O_3—C loadings produced a 1:2 Al_2O_3:C stoichiometry because of the preferential formation of CO_2 over CO. The Cl_2 flow rates were selected to provide required reactor holdup times as determined from earlier studies (Dobbins, 1986).

Table 1. Variable Levels for the Variable Screening Experiment

Parameter	High (+)	Low (−)
Temperature, K	1,073	873
NaCl:$AlCl_3$ molar ratio	48:52	40:60
Melt:Al_2O_3 ratio (wt.)	7.5:1	15:1
Melt:C ratio (wt.)	21:1	42:1
Cl_2 flow rate, m^3/s	4.1×10^{-6}	1.5×10^{-6}

Combinations of experimental parameters used in each of the eight experiments are listed in Table 2, along with the steady-state chlorination rate of Al_2O_3 for each experiment. The steady-state rate was defined by extrapolating the observed reaction rate between 30 and 90 minutes back to time zero.

A variable was considered statistically significant if its effect was greater than that of the average effect of the two dummy variables, which was 0.40. The dummy variables were not experimental parameters, but specific combinations of experiments that could have been assigned an independent variable as part of the test, but were not. Since these combinations of experiments correspond to a nonexistent or "constant" parameter, the variation calculated from these combinations is actually a measure of the experimental error (Stowe and Meyer, 1966). Replication of a particular set of experimental conditions would have been another technique of estimating the experimental variance. The plus-minus combinations corresponding to the two dummy variables may be determined by extending the pattern shown in Table 2 to the right for parameters 6 and 7 (not shown).

Of the five parameters tested, temperature was the only one found to be statistically significant. Melt:Al_2O_3 ratio had the least effect on the reaction rate; reaction was zero order in Al_2O_3 for conversions as high as 95%. If the reaction rate were at all influenced by processes occurring at the Al_2O_3 surface, there should have been a change in reaction rate with the loss of surface area resulting from Al_2O_3 conversion. The lack of rate dependence indicates that: 1) a dissolved species was being chlorinated and 2) the Al_2O_3 dissolution rate was much faster than the chlorination rate.

A second variable, melt composition, would be expected to influence both the solubility and dissolution rates of Cl_2 and Al_2O_3. However, no significant rate changes were observed with changes in melt composition. The dissolution rate of the oxide must have, therefore, been fast enough at the test conditions to

Table 2. Reaction Rates and Conditions for the Plackett-Burman Experimental Design

Trial No.	Parameter No. & Level					Reaction Rate of Al_2O_3 kmol/s × 10^8
	1	2	3	4	5	
1	+	+	+	−	+	2.00
2	+	+	−	+	−	1.83
3	+	−	+	−	−	1.77
4	−	+	−	−	+	0.38
5	+	−	−	+	+	2.78
6	−	−	+	+	+	0.75
7	−	+	+	+	−	0.72
8	−	−	−	−	−	0.33
Effect*	0.93	0.11	0.02	0.24	0.19	

*An effect greater than 0.40 is statistically significant at the 95% confidence level.

mask any solubility difference. Also, there was no measurable effect on the solubility and transport of Cl_2. The solubilities of Al_2O_3 in $40\%_m$ and $48\%_m$ $AlCl_3$ melts at the reaction temperatures were estimated to be $0.80\%_w$ and $0.23\%_w$, respectively (Dobbins, 1986) based on solubilities reported for lower temperatures (Tremillion, 1976; Seon, 1983).

The effect of C loading and of Cl_2 flow on reaction rate was also found to be statistically insignificant. However, closer examination of the experimental results indicated that, in spite of the Plackett-Burman results, melt:C ratio did have an effect on chlorination rate. At fixed combinations of temperature and Cl_2 flow rate (trial pairs 1-5, 2-3, 4-6, and 7-8), high C loadings (low melt:C ratios) produced higher reaction rates than low C loadings. Differences in Al_2O_3 loadings and melt compositions were ignored since these variables did not affect the reaction. At 873 K, the change was proportional to the C loading while at 1,073 K it was not.

An exception to the above was trial pair 2-3, where both rates were approximately the same. In trial 2, 100% Cl_2 conversion was attained, which limited the observable chlorination rate to the Cl_2 flow. An increased chlorination rate in trial 2 (i.e., not Cl_2-limited) would have resulted in a greater significance for the melt:C parameter. The apparent insignificance of C loading in the Plackett-Burman study was thus a result of the choice of experimental parameters rather than a physical or chemical phenomenon.

Temperature effects

To better define the temperature dependence of the reaction, a series of chlorinations were carried out between 803 and 1,073 K. Experimental conditions used were:

Melt:Al_2O_3 ratio (wt.)	7.5:1
Melt:C ratio (wt.)	21:1
Cl_2 flow rate, m^3/s	4.1×10^{-6}
Melt composition at 873 K and above	$40\%_m$ $AlCl_3$-$60\%_m$ NaCl
Melt composition at 823 K and below	$45\%_m$ $AlCl_3$-$55\%_m$ NaCl

Two melt compositions were used to alleviate a problem with NaCl precipitating from the melt and plugging the Cl_2 sparger. This change did not affect the measured reaction rate, since the rate was not influenced by Al_2O_3 dissolution or Cl_2 transport.

Figure 2 shows the reaction rate as a function of time for chlorinations at 803, 823 and 873 K. All three experiments exhibited the same basic behavior, an initially high reaction rate followed by a decline over the next 30 to 45 minutes to a virtually constant rate. The initial decrease in rate with time cannot be adequately explained by a loss of C surface area since the maximum observed C conversion over the first 45 minutes of reaction was only $3\%_w$. Total C conversions for these three runs after 80 minutes ranged from $2.3\%_w$ at 803 K to $6.9\%_w$ at 873 K.

The reaction rates vs. time data for chlorinations at 973, 1,023 and 1,073 K are given in Figure 3. These three profiles are quite similar as a group, but significantly different from the low-temperature profiles in Figure 2. Instead of an initial burst of reaction followed by a decline, these experiments have relatively constant reaction-rate/time profiles in which the reaction rate drops by about 10% over a 150-minute period. The decrease in reaction rate in the high-temperature experiments is thought to be related to changes in C surface area with conversion. Total C conversions were 17.3, 21 and $25\%_w$ at 973, 1,023 and 1,073 K, respectively.

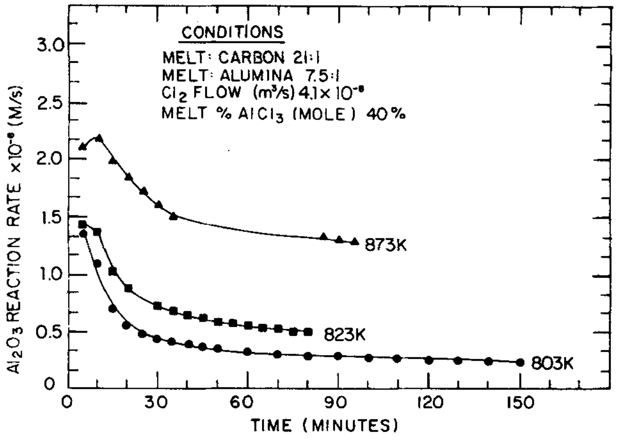

Figure 2. Reaction rate profiles for the chlorination of Al_2O_3 at $\leq$873 K.

The overall temperature dependence of the chlorination is best described by the Arrhenius plot shown in Figure 4. The activation energy for chlorination below 923 K is 121 kJ/kmol, significantly larger than the 29.4 kJ/kmol for chlorination in the region from 973 to 1,073 K. The activation energies for the high- and low-temperature regions are consistent with values expected for mass transfer and kinetic control, respectively.

Further evidence of a kinetically controlled reaction below 923 K is the effect of C loading on the rate as revealed by the Plackett-Burman experiments. At low temperatures, doubling the carbon loading produced a corresponding increase in the reaction rate from an average of 0.36×10^{-8} to 0.74×10^{-8} kmol/s (trials 4 and 8 vs. 6 and 7).

A similar increase in reaction rate is noted between Plackett-Burman trial 7 and the 873 K temperature dependence experiment, which were identical runs except for the C source. The ratio of the surface area of the coke used in the Plackett-Burman study to that used in the temperature dependence experiments was 0.473 as determined from particle-size distributions. This

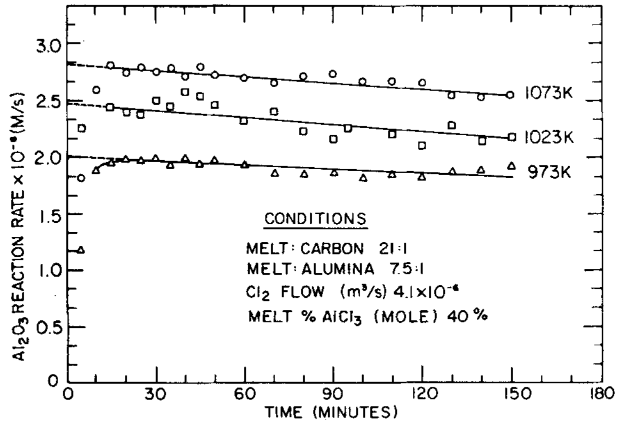

Figure 3. Reaction rate profiles for the chlorination of Al_2O_3 at $\geq$973 K.

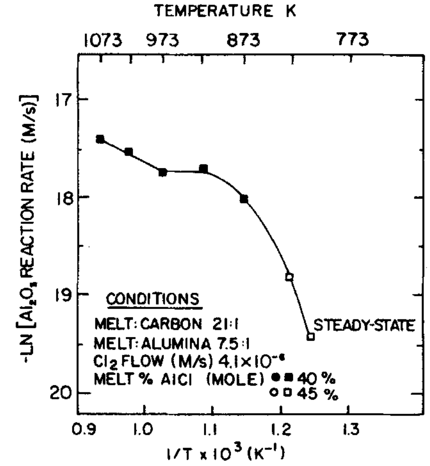

Figure 4. Arrhenius plot for the reaction of Al_2O_3.

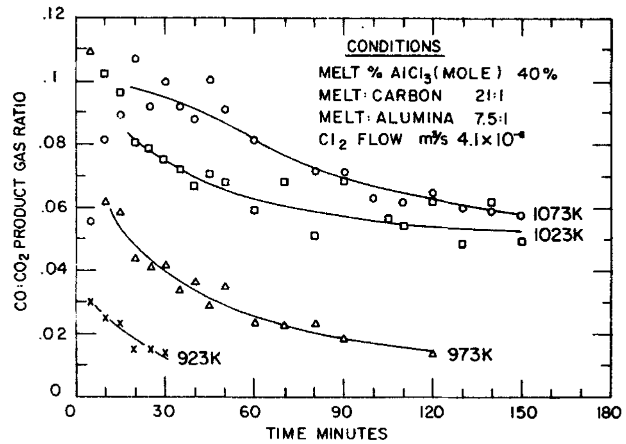

Figure 5. Ratio of CO to CO_2 for the chlorination of Al_2O_3 at ≥923 K.

ratio is very close to the 0.5 ratio observed experimentally between the reaction rates.

Turning to the high-temperature runs, the evidence in support of gas-liquid mass transfer being the rate-limiting step is the lack of a difference in reaction rate between the corresponding Plackett-Burman 5 experiment and the temperature dependence experiment at 1,073 K. Mass transfer control was confirmed by experiments to test the effect of C loading at 973 K which showed that the reaction rate was insensitive to C loading and that both the gas holdup in the reactor and the reaction rate were proportional to the stirring speed (Dobbins, 1986).

The experiments on the effect of C loading at 1,023 K showed that at melt:carbon loadings of less than 21:1 (Al_2O_3:melt ratio constant at 7.5:1) the Al_2O_3 reaction rate was constant at 1.41×10^{-8} kmol/s. As the C loading was increased to a melt:carbon ratio of 8.3:1, the reaction rate increased to 2.15×10^{-8} kmol/s. This behavior is contrary to what would have been expected if the reaction were kinetically controlled at the C surface, where the reaction rate would increase as C loading was increased at low levels and then become constant once mass transfer became limiting. It is thus evident that the C:Al_2O_3 ratio has an important effect on gas:liquid mass transfer but further work is required to fully determine the nature of the interaction.

Carbon reaction

The inflection point in the 923 to 973 K region of the steady-state reaction curve (Figure 4) has also been reported by previous investigators and attributed to the instability of $COCl_2$, an important reaction intermediate (Podor et al., 1982; Goken, 1984). Evidence of a similar effect also due to $COCl_2$ is found in Figure 5, a plot of the CO:CO_2 ratio in the product gas as a function of time. At temperatures below 923 K, CO was not detectable at all, while above 923 K both the absolute level of CO and the CO:CO_2 ratio increased with temperature. The lack of CO in the product gas at low temperatures and the maxima in the reaction rate at 923 K strongly suggest the presence of $COCl_2$ as an integral part of the reaction mechanism.

Figure 5 shows another characteristic of fused salt chlorination, high CO_2 yields. If the Boudard reaction,

$$C + CO_2 \leftrightarrow 2CO \tag{7}$$

were to reach equilibrium at 1,073 K, the CO:CO_2 ratio would be 11 not 0.1. The low CO:CO_2 ratio indicates that oxygen or CO is captured on the C surface as a part of the reaction mechanism. If free CO were formed as part of the reaction, it would not be expected to remain in the reactor long enough to form $COCl_2$ at 100% conversion levels, which is what would be required to explain the lack of CO at low temperatures. This leads to the conclusion that the reaction must occur in such a manner that partially oxidized C atoms remain bonded to the C matrix.

The decrease in CO:CO_2 ratio with time at temperatures above 973 K, ranging from 25 to 60% of the initial value, without a corresponding decrease in the reaction rate is best explained by a change in C surface reactivity with conversion. If the CO in the product gas resulted strictly from the dissociation of $COCl_2$ formed as a reaction intermediate, then the CO:CO_2 ratio should be constant. Since this is not the case, CO must be generated (at least in part) by thermal desorption of CO from the C surface.

A heterogeneous material such as coke would be expected to contain a variety of C structures, each with its own reactivity. The resulting reaction sites would also explain the similarity between the low-temperature reaction rate profiles and the CO:CO_2 ratios shown in Figure 5. The more reactive sites would be responsible for both the high starting rates at low temperatures and the high initial product gas CO levels at high temperatures. As the C would be consumed and its surface depleted of these highly reactive sites, the overall reactivity of the coke would fall off until a steady-state condition was reached.

Mixed Oxide Chlorination

In the case of a mixed oxide such as fly ash, the surface is non-homogeneous but very large, which tends to assure oxide availability in proportion to the concentrations present. Thermodynamically, all of the major oxides in fly ash, with the exception of SiO_2, are capable of undergoing both carbochlorination and the exchange reaction with $AlCl_3$. However, different melt compositions would be expected to influence the fly ash-melt reactions and hence the chlorination rate.

To demonstrate the effect of melt composition, runs were made at $40\%_m$ $AlCl_3$-$60\%_m$ NaCl and at $48\%_m$ $AlCl_3$-$52\%_m$

NaCl. The two runs were designated as 40A and 48A, respectively. The other experimental conditions were held constant at:

Temperature, K	1,023
Melt:C ratio (wt.)	21:1
Melt:fly ash ratio (wt.)	42:1
Cl_2 flowrate, m^3/s	4.1×10^{-6}

The fly ash was added to the reactor 10 minutes before the Cl_2 was started. Because of this time differential, the ash-melt exchange reaction started slightly before the carbochlorination reaction. Slurry samples were taken at 15-minute intervals. The 40A experiment was terminated after 62.5 minutes and the 48A experiment after 180 minutes.

Silicon, Al and Fe oxides are the major components of fly ash, making up 47.6, 32.3 and 10.4%$_w$ of the Halomet ash, respectively. The remainder consists of relatively reactive alkali, alkaline earth, and other trace metal oxides, which tend to be trapped in the glassy portion of the ash matrix (Hulett and Weinburger, 1981) and, therefore, follow the chlorination of Si in the ash (Dobbins, 1984). Figures 6 and 7 show the conversion of Si, Al and Fe oxides vs. time for the 40A and 48A runs, respectively. It should be kept in mind that these curves reflect both the effect of chlorination and of dissolution of the oxide in the melt.

Some conversion of the ash occurred before Cl_2 to the reactor was turned on, Figures 6 and 7. Production of $FeCl_3$ took place almost immediately as evidenced by the appearance of yellow condensate in the upper portion of the reactor and in the first condenser. Silicon and aluminum oxides removed from the ash in this initial period are believed to form $SiCl_4$ and $AlOCl_2^-$, respectively, although no direct proof of this is available. The concentration of $SiCl_4$ in the melt at any particular time would be expected to be extremely small because of the chloride's low boiling point.

The conversion of iron oxide is virtually identical for the two runs, as would be expected since Fe_2O_3 reacts readily with $AlCl_3$. The similarity serves to verify that the differences observed in the SiO_2 and Al_2O_3 conversion rates are not artifacts caused by errors in slurry sampling. In 40A the conversion of both SiO_2 and Al_2O_3 occurs quite rapidly between 7.5 and 22.4 minutes and then levels off, while in 48A the SiO_2 and Al_2O_3 conversion rates are virtually constant throughout. As a consequence, the total amount of oxide chlorinated during the first 50 minutes of reaction is roughly equal for the two runs, although there is a significant difference in the Al_2O_3:SiO_2 conversion ratio. After 30 minutes of reaction, the conversion rate of Al_2O_3 for 48A is 1.3 times that of 40A and the rate for SiO_2 is 3.6 times greater, giving a much faster overall conversion of the ash, but with much less selectivity between SiO_2 and Al_2O_3.

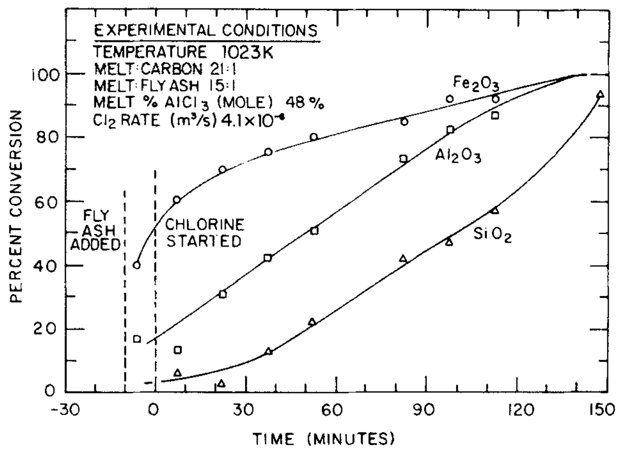

Figure 7. Conversion rates of Fe, Al and Si oxides in Halomet nonmagnetic ash at 1,023 K in a 48% $AlCl_3$ melt.

In addition to monitoring the chlorination that is taking place by analyzing samples of the melt, gas chromatography was used to follow the CO_2 content of the product gas. Figure 8 is a plot of the measured CO_2 production vs. time for both runs. Run 40A shows a greater initial CO_2 production rate than does 48A, which is in agreement with the oxide conversion data. Carbon monoxide levels accounted for less than 2%$_w$ of the total C conversion. The total amount of CO and CO_2 produced was within 3%$_w$ of that predicted from the oxide conversions.

Although the total carbon oxide production agreed with the oxide conversion data for both runs, the rate at which it was produced did not. In the first 30 minutes of reaction, the CO_2 production rate in 40A, based on oxide conversions, should have

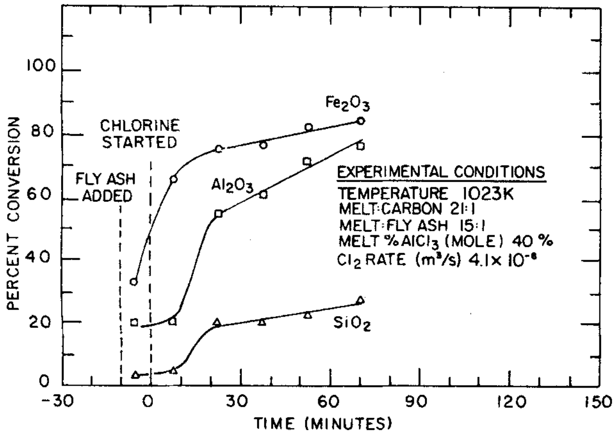

Figure 6. Conversion rates of Fe, Al and Si oxides in Halomet nonmagnetic ash at 1,023 K in a 40% $AlCl_3$ melt.

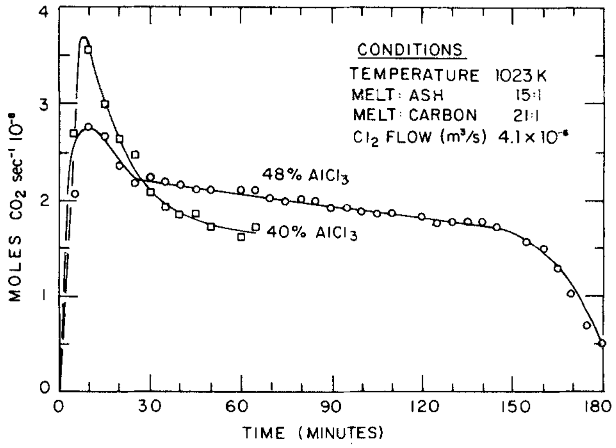

Figure 8. Carbon dioxide production rates for Halomet nonmagnetic ash in 40% and 48% $AlCl_3$ melts.

averaged 7×10^{-8} kmol/s. The observed rate was 4.8×10^{-8} kmol/s. In the last 30 minutes of reaction the trend was reversed; the actual rate was 3.0×10^{-8} kmol/s compared to the oxide-based rate of 1.7×10^{-8} kmol/s. In 48A the same trend was observed but the differential was much less. In the first 30 minutes the actual average rate was 4.3×10^{-8} kmol/s compared to an oxide rate of 4.5×10^{-8}, while from 30 to 60 minutes the average rates were 3.7×10^{-8} kmol/s actual vs. 3.2×10^{-8} kmol/s from the oxide data.

The differences between the oxide conversion and actual CO_2 production rates indicate that at the start of 40A the reaction at the C surface was slower than the dissolution rate of the oxide into the melt. The same was true for 48A, but the difference was significantly smaller. Tremillion et al. (1976) have shown that the solubility of oxides in NaCl—$AlCl_3$ melts goes through a minimum at compositions near equimolar, which would explain these results. The high rates of oxide conversion between 7.5 and 22.5 minutes in 40A result primarily from enhanced solubility.

Another difference between the chlorination of fly ash and of Al_2O_3 is the maximum chlorination rate, as measured by CO_2 production. The fly ash chlorinations should have been rate-limited by gas-liquid mass transfer with an expected CO_2 production rate of 4.25×10^{-8} kmol/s based on the chlorination of Al_2O_3. However, both 40A and 48A exceeded this value for the first 30 minutes, the 40A run by over 50%. This is attributed to $FeCl_3$ produced from the ash enhancing the transport of Cl_2 by the following reaction (Bezukladnikov et al., 1974):

$$FeCl_3 \rightarrow 0.5\,Cl_2 + FeCl_2 \tag{8}$$

This reaction would be favored in an $AlCl_3$-lean melt, since $FeCl_3$ can become a complex with NaCl. The formation of such a complex would explain why the chlorination rate of 40A is higher than 48A relative to Al_2O_3 (as measured by CO_2 production).

That the chlorination rate in both 40A and 48A was ultimately limited by the dissolution rate of the ash rather than gas-liquid mass transfer was confirmed by the drop in CO_2 production to 3.75×10^{-8} kmol/s, which is less than that observed for Al_2O_3 chlorination at the same operating conditions after 30 minutes of reaction. Also, the observed CO_2 production rates at 30 minutes were less than the rates predicted from the oxide conversions for both runs, which is further evidence of dissolution control.

Although the amount of oxides dissolved was greater for the $40\%_m$ $AlCl_3$ melt, the $48\%_m$ $AlCl_3$ melt was much more aggressive in attacking the entire ash matrix. During the first 50 minutes of chlorination, the ratio of SiO_2 to Al_2O_3 conversion was 5.46 compared to 2.55 for 48A over the same period of time. In terms of overall ash conversion, the two chlorinations were approximately equal; 0.37 for 40A and 0.34 for 48A. The reduced selectivity of the 48%m $AlCl_3$ melt is the result of the reaction:

$$NaAlCl_4 \rightarrow NaCl + AlCl_3 \tag{9}$$

As the concentration of $AlCl_3$ in the melt is increased, more free $AlCl_3$ is produced. This free $AlCl_3$, although slightly more stable thermodynamically ($G < 40$ kJ/kmol) than SiO_2 at the reaction temperatures, is more capable of reacting with SiO_2 than with $NaAlCl_4$, which is approximately 100 times more stable than SiO_2 (Dobbins, 1986). The exchange reaction for SiO_2 is:

$$4AlCl_3 + 3SiO_2 \leftrightarrow 2Al_2O_3 + 3SiCl_4 \tag{10}$$

Because of the high vapor pressure of $SiCl_4$ at 600 K and above ($SiCl_4$ boils at 330 K), $SiCl_4$ formed by Eq. 10 would not be expected to remain in the reactor. For this reason, the equilibrium condition predicted by thermodynamic analysis and shown in Eq. 10 would never be established. This discussion explains why melt composition has an effect on SiO_2 conversion. It also shows that SiO_2 would be expected to follow an exchange reaction path as opposed to forming a soluble oxychloride and reacting at the C surface.

The relative merits of high or low selectivity between SiO_2 and Al_2O_3 chlorination is a process question that is beyond the scope of this paper. It is important to note, however, that selectivity is a strong function of melt composition that is itself strongly influenced by process conditions, primarily temperature. Higher operating temperatures will tend to favor using melts of lower $AlCl_3$ content.

Conclusions

The mechanism and kinetics have been determined for the recovery of the metal oxides in a polymetallic ore (power plant fly ash) by carbochlorination. The solid reactants were suspended in a NaCl-$AlCl_3$ melt into which Cl_2 was sparged at 803 to 1,073 K. The molten salt medium acted as a solvent for the oxides. The dissolved oxide species then reacted with the molten salt or with the C and Cl_2 to produce volatile metal chlorides that can be recovered and separated.

The process was successfully demonstrated using the carbochlorination of pure alumina, the rate of which was found to be chemical-reaction-controlled at temperatures below about 923 K and gas-liquid mass transfer controlled at higher temperatures. The carbochlorination rate for the mixed oxides in the ash was also mass-transfer-controlled at higher temperatures when Al recoveries were less than about 50%. At higher Al recoveries, the overall rate was limited by the rate of ash dissolution into the melt.

Acknowledgment

This work was supported by the U.S. Department of Energy, contract No. W-7405-Eng-82 and in part by the Iowa State Mining and Mineral Resources Research Institute under U.S. Bureau of Mines Allotment Grants G1144119 and G1154119. The authors wish to thank M. J. Murtha for helpful suggestions throughout the investigation.

Notation

G = total Gibbs free energy
w = by weight
m = by mole

Literature Cited

Adelman, D. J., and G. Burnet, "Carbochlorination of Metal Oxides with Phosgene," *AIChE J.*, **33**, 64 (1987).

Bamberger, C. E., "Experimental Techniques in Molten Fluoride Chemistry," in the "Advances in Molten Salt Chemistry," Vol. 3, J. Braunstein, G. Mamantov, and G. P. Smith, eds., Plenum Press, New York (1975).

Bezukladnikov, A. B., E. Ya Tarat, and D. P. Baibakov, "Rate of Absorption of Chlorine and Mechanism of its Transfer in Melts Containing Iron Chlorides," *Z. Prikl. Khim.*, **47**(8), 1722 (1974).

Bombara, G., and R. Tanzi, "Prospects for Carbochlorination in Aluminum Recovery from Italian Leucites," *J. Met.*, **36**, 74 (1984).

Burnet, G., M. J. Murtha, and J. W. Dunker, "Recovery of Metals from Coal Ash—an Annotated Bibliography," USDOE IS-4833 (rev.), UC-90, Ames Laboratory, Ames, IA (1984).

Dobbins, M. S., "Carbochlorination of Metal Oxides Using a Fused Salt Slurry Reactor," Ph.D. Dissertation, Iowa State Univ., Ames, IA (1986).

Dobbins, M. S., and G. Burnet, "A Molten Salt Reactor for Dispersed Solid Phase Chlorination," AIChE Mtg., San Francisco (Nov. 25–30, 1984).

Goken, N. A., "Rates of Chlorination of Aluminous Resources," Bureau of Mines I.C. 8952 (1984).

Haupin, W. E., and J. A. Remper, M. B. Dell, "Production of Aluminum Chloride," U.S. Patent #4,039,648 (Aug. 2, 1977).

Hille, J., and W. Durrwachter, "Manufacture of Anhydrous Aluminum Chloride from Alumina in the Vortex Layer," *Angew. Chem.*, **72**, 850 (1960).

Hulett, L. D., A. J. Weinburger, K. J. Northcutt, and J. Fergesun, "Chemical Species in Fly Ash from Coal-Burning Power Plants," *Sci.*, **210**, 1356 (1981).

Milne, D. J., and R. D. Holliday, "Thermodynamics of Gas-Solid Reactions for Purification of Bauxite," *Ind. Eng. Chem., Process Des. Dev.*, **14**(4), 442 (1975).

Podor, B., and I. Bertoti, "Mass Spectrometric Investigation of Gamma-Alumina Chlorination by Carbon Tetrachloride," *Thermochim. Acta.*, **56**, 209 (1982).

Seon, F., G. Picard, and B. Tremillion, "Industrial Aluminas and Hexahydrated Aluminum Chloride Chlorinations by Phosgene in LiCl-KCl Eutectic Melt at 470°C," *Electrochim. Acta.*, **28**(2), 209 (1983).

Stowe, R. A., and R. P. Meyer, "Efficient Screening of Process Variables," *Ind. and Eng. Chem.*, **58**(2), 36 (1966).

Tremillion, B., A. Bermone, and R. Molina, "Electrochemistry in Molten $NaAlCl_4$ (at 210°C): Identification of Dissolved Oxide Containing Species, Solubility of Alumina in terms of pCl^- and Properties Related to H_2O in This Melt," *J. of Chem. and Eng. Data*, **23**(2), 53 (1976).

Manuscript received Oct. 1, 1987, and revision received Apr. 4, 1988.